An analytical method to estimate groundwater depletion of an aquitard due to variable drawdowns in adjacent aquifers

Zhaofeng Li[1], Hao Li[1], Xianxuan Xiao[2], Walter A Illman[2], and Ruizhe Wang[2]

[1]College of Environment and Civil Engineering, Chengdu University of Technology
[2]Chengdu University of Technology

November 23, 2022

Abstract

Computing aquitard depletion, which is often overlooked, is of great significance for the assessment of groundwater resources and land subsidence. The issue is viewed as troublesome because of the additional computational burden, the poorly known hydrogeological parameters of the aquitard, and the lack of drawdown history in pumped aquifers. In this study, an analytical solution is derived to describe the drawdown variation in a nonlinear-consolidated aquitard under the condition of variable drawdowns in adjacent aquifers. Based on the analytical solution, we study the characteristics of groundwater dynamics and water balance under the conditions of linearly increasing drawdown of aquifers in adjacent aquifers. In addition, we put forward a method to calculate the depletion and hydrogeological parameters of an aquitard corresponding to variable drawdowns in adjacent aquifers, applicable even when historical drawdown data are lacking. The accuracy of the method is generally very good, but results improve when the drawdown history of pumped aquifers is divided into more periods for estimation. Under the condition of linear drawdown in adjacent aquifers, groundwater depletion and maximum water release rate of the aquitard increases with increasing compression index, coefficient of consolidation, aquitard thickness, rate of drawdown change in the adjacent aquifer, while decreasing with initial void ratio, and initial effective stress. The proposed approach is demonstrated at a field site in Shanghai City of China, and it would help for the effective management of groundwater resources and estimation of the global transfer from groundwater to surface water.

An analytical method to estimate groundwater depletion of an aquitard due to variable drawdowns in adjacent aquifers

Zhaofeng Li [1, 2, 3] *, Hao Li [1], Xianxuan Xiao [1, 2,] , Walter A. Illman [3], and Ruizhe Wang [1]

[1] College of Environment and Civil Engineering, Chengdu University of Technology, Chengdu 610059, China

[2] State Key Laboratory of Geohazard Prevention and Geoenvironment Protection (Chengdu University of Technology), Chengdu 610059, China

[3] Department of Earth & Environmental Sciences, University of Waterloo, Waterloo, Ontario, Canada

Corresponding author: Zhaofeng Li (lizhaofeng17@cdut.edu.cn)

Key points:

• Analytical solution of drawdown in an aquitard corresponding to variable drawdowns is derived.

• An analytical method to estimate groundwater depletion from an aquitard is proposed.

• Corresponding type-curve fitting method is developed to estimate hydraulic parameters.

• Analysis of factors contributing to aquitard deformation is presented.

Keywords: Nonlinear consolidated aquitard; Groundwater depletion; Variable drawdowns; Type-curve fitting method; Groundwater storage assessment

Abstract

Computing aquitard depletion, which is often overlooked, is of great significance for the assessment of groundwater resources and land subsidence. The issue is viewed as troublesome because of the additional computational burden, the poorly known hydrogeological parameters of the aquitard, and the lack of drawdown history in pumped aquifers. In this study, an analytical solution is derived to describe the drawdown variation in a nonlinear-consolidated aquitard under the condition of variable drawdowns in adjacent aquifers. Based on the analytical solution, we study the characteristics of groundwater dynamics and water balance under the conditions of linearly increasing drawdown of aquifers in adjacent aquifers. In addition, we put forward a method to calculate the depletion and hydrogeological parameters of an aquitard corresponding to variable drawdowns in adjacent aquifers, applicable even when historical drawdown data are lacking. The accuracy of the method is generally very good, but results improve when the drawdown history of pumped aquifers is divided into more periods for estimation. Under the condition of linear drawdown in adjacent aquifers, groundwater depletion and maximum water release rate of the aquitard increases with increasing compression index, coefficient of consolidation, aquitard thickness, rate of drawdown change in the adjacent aquifer, while decreasing with initial void ratio, and initial effective stress. The proposed approach is demonstrated at a field site in Shanghai City of China, and it would help for the

effective management of groundwater resources and estimation of the global transfer from groundwater to surface water.

1. Introduction

Groundwater is generally overexploited over the world due to the increasing demand for water resources, and it has brought a series of environmental problems, including the decline of groundwater levels, land subsidence (Li et al., 2021; Shi et al., 2007; Shi et al., 2008) and sea level rise (Konikow & Kendy, 2005). A multi-layered aquifer system in the sedimentary plain area, such as the Dakota aquifer system in the United States and the Yangtze Delta in China (Guo & Li, 2015; Ye et al., 2016), usually consists of multiple aquifers with alternating aquitards in between (Zhuang et al., 2015). Water stored in aquitards is a significant source of pumped aquifers, and it tends to be more storable than confined aquifers (Liu et al., 2022; Zhang et al., 2020a). Meanwhile, aquitard storage is difficult to recover and could often be the primary source of groundwater released from the storage of aquifer systems (Shi et al., 2008). Consequently, the accurate calculation of groundwater depletion in aquitards is essential for the effective management of groundwater resources, and it would help estimate the global transfer of groundwater to surface water (Konikow & Neuzil, 2007).

Due to low hydraulic conductivity and non-negligible specific storage, water release from aquitards and its deformation always lag behind the drawdown in adjacent confined aquifers (Bakr, 2015; Liu et al., 2022; Ye et al., 2016). Zhou et al. (2013) studied the groundwater dynamics and water balance of an aquitard, while the drawdown was a constant amount in an adjacent confined aquifer. The hydraulic head in aquifers lying above or under the aquitard usually decreased with increasing groundwater extraction (Custodio, 2002), Neuman & Gardner (1989) presented convolution integrals for calculating the drawdown in the aquitard under the condition of water table fluctuation. A widely applicable method was proposed to estimate the groundwater depletion of the aquitard in the entire or limited period of exploitation history, especially when the data on drawdown of history is sufficient (Li & Zhou, 2015; Li et al., 2017). Konikow & Neuzil (2007) presented a simplified method to estimate the groundwater depletion from the confining layers in response to withdrawals from adjacent aquifers. Alternatively, given the same information, a well-calibrated, numerical simulation model (i.e., three-dimensional model such as MODFLOW can be used to compute the groundwater depletion of aquitards in response to pumping of aquifers (Arabameri et al., 2020; Burbey, 2020; Zhang et al., 2020b).

Most of the aforementioned studies were carried out based on the one-dimensional consolidation theory for saturated clays (Terzaghi, 1943), which assumed the aquitard hydraulic parameters being constant values. However, in reality, hydraulic parameters decrease nonlinearly during the consolidation process of the aquitard, which is contrary to the assumption of Terzaghi's theory, and Terzaghi's model often leads to unexpected differences between theoretical results and field observations (Davis & Raymond, 1965; Gibson et al., 1967; Xie & Leo, 2004). Li et al. (2018) and Luo et al. (2020) proposed analytical solutions to characterize the water release from a one-dimensional large-strain aquitard and a nonlinearly consolidated aquitard, respectively, subjected to an abrupt hydraulic head decline in adjacent confined aquifers.

The accuracy of water depletion calculation of the aquitard storage relies to a large degree on the accuracy of aquitard hydraulic parameters, which can be determined by the results of laboratory and in-situ experiments (Burbey, 2020; Zhang et al., 2020b; Zhao et al., 2019). Zhou et al. (2013) used an analytical method to calculate aquitard hydraulic parameters while the drawdown in the adjacent aquifer was constant. Burbey (2003) characterized the specific storage and hydraulic conductivity of the aquitard by taking advantage of time-subsidence data during a pumping test with a graphical technique. (Zhang et al., 2015); Zhuang et al. (2015) proposed a type-curve method for estimating the hydraulic conductivity and the specific storage of an aquitard in a multi-layered aquifer system by using data on aquitard compaction and drawdown history of aquifers. Luo et al. (2020) calculated the hydraulic parameters of the aquitard undergoing non-linear consolidation using a laboratory experiment while the drawdown in the adjacent aquifer was constant. In addition, Konikow & Neuzil (2007) demonstrated a general relationship between porosity and hydraulic conductivity considering the clay content of the aquitard and the relation between porosity and specific storage considering the consolidation degree.

In short, it is difficult to calculate the water depletion of the aquitard because of the complex drainage process and poorly known hydraulic parameters of the aquitard, and the paucity of drawdown data within the pumped aquifer, especially during the early stage of groundwater exploitation and in developing countries. In this study, we present an analytical solution to describe the drawdown in an aquitard for an arbitrary drawdown of adjacent confined aquifers. Based on the analytical solution, we also develop methods to calculate the hydrogeological parameters and the long-term decreases in the volume of water stored in an aquitard undergoing nonlinear consolidation, under a condition that the drawdown history of the aquifers lying above and below the aquitard can be approximated as a step-by-step piecewise function with respect to time, in each of which the drawdown is a constant amount. The new method proposed in this study is demonstrated through a laboratory experiment and a field application to the aquifer system beneath Shanghai city of China. The hydraulic parameters determined by the method in this study are compared with the geological method of Konikow & Neuzil (2007). The results of the laboratory experiment and field applications demonstrate the correctness and accuracy of the approach in this study.

2. Mathematical Model and Analytical Method

2.1 The Governing Equation of Drawdown in the Aquitard

Hydraulic head in an aquifer alters the boundary conditions for the adjoining aquitard, causing it to release water from storage to the aquifer as drawdown propagates slowly into the aquitard. Despite the low permeability nature of aquitards, relatively large specific storage values in clay-rich aquitards can enable large quantities of water to ‘‘leak’’ into aquifers over long timescales (Konikow & Neuzil, 2007). To study the water amount released from the aquitard, a multi-layered aquifer system was considered. The Lagrangian coordinate a was used, which was assumed to be positive in a vertically downward direction, with the coordinate origin located at the top surface of the aquitard (Figure 1).

The system is composed of an aquitard and aquifers on both sides, of which horizontal length is infinite. The hydraulic conductivity of each aquifer exceeds that of the aquitard by at least two orders of magnitude. As seepage in the aquitard follows the path of least resistance, water flow in the confining layer is essentially vertical (Neuman & Gardner, 1989; Neuman & Witherspoon, 1969; Zhang et al., 2015).

Figure 1. Conceptual model of the multi-layered aquifer-aquitard system.

The assumptions of one-dimensional nonlinear consolidation theory are as follows: (1) The horizontal length of the aquitard is infinite and its initial thickness is l; (2) the aquitard is homogeneous and saturated; (3) individual clay particles and the pore water in the aquitard are incompressible during consolidation; (4) the groundwater flow in the aquitard is one-dimensional, vertical and follows Darcy's law; (5) soil creeping is not considered, and the nonlinear variations of aquitard compressibility during the consolidation process are assumed to abide by equation (1).

$$e = e_0 - C_c \log_{10}(\sigma' / \sigma_0') \#(1)$$

where the soil compression index C_c is assumed to be constant (dimensionless), and is approximately valid; e is the void ratio in the aquitard at position a and time t (dimensionless); e_0 is the initial void ratio of the aquitard (dimensionless); σ' is the vertical effective stress ($ML^{-1}T^{-2}$); and σ_0' is the initial effective stress ($ML^{-1}T^{-2}$). (6) The coefficient of aquitard compressibility (m_v) can be given by:

$$m_v = -\frac{1}{1+e}\frac{de}{d\sigma'} = \frac{0.434C_c}{(1+e)\sigma'} \#(2)$$

where the change of (1+ e) with time during the consolidation process is much smaller than the σ', so for any load increment, (1+ e) can be regarded as a constant (Luo et al., 2020). Because the variation of e is much smaller than the variation of σ', the coefficient of consolidation c_v is considered to be relatively constant (Davis & Raymond, 1965). This is equivalent to assuming that the decrease in m_v is proportional to the decrease in hydraulic conductivity k_v during the consolidation process of the aquitard.

$$c_v = \frac{k_v}{m_v\gamma_w} \#(3)$$

where, γ_w is unit weight of water.

A nonlinear large deformation consolidation equation (Gibson's theory) with a void ratio as control variable is given by Gibson et al. (1967); (Gibson et al., 1981), while the self-weight of the soil is ignored (Luo et al., 2020).

$$\frac{\partial}{\partial a}\left[\frac{k_v(1+e_0)}{\gamma_w(1+e)}\frac{d\sigma'}{de}\frac{\partial e}{\partial a}\right] + \frac{1}{(1+e_0)}\frac{\partial e}{\partial t} = 0 \#(4)$$

Substituting equations (1), (2) and (3) into equation (4) to obtain the governing equation of depletion of the aquitard undergoing nonlinear consolidation:

$$c_v\left[\frac{\partial^2\sigma'}{\partial a^2} - \frac{1}{\sigma'}\left(\frac{\partial\sigma'}{\partial a}\right)^2\right] = \frac{\partial\sigma'}{\partial t} \#(5)$$

In addition, according to the principle of effective stress(Terzaghi, 1943),

$$\sigma' = \sigma_0' + \gamma_w s\#(6)$$

where s is the drawdown in adjacent aquifers.

For the thin soil layer, the weight of the soil layer can be ignored, and the initial effective stress (σ_0', geostatic stress) is distributed uniformly through the entire thickness, and the accuracy of calculation is poor while the thickness of aquitard is large (Gibson et al., 1967; Gibson et al., 1981). Substituting equation (6) into equation (5) leads to a governing equation describing nonlinear consolidation of an aquitard.

$$c_v\left[\frac{\partial^2 s}{\partial a^2}-\frac{\gamma_w}{\sigma_0'+\gamma_w s}\left(\frac{\partial s}{\partial a}\right)^2\right]=\frac{\partial s}{\partial t}\#(7)$$

It is assumed that the initial drawdown distribution in the aquitard is a function $f(a)$ of position a, which is caused by a previous external force disturbance, and the drawdown in the aquifers lying above and under the aquitard are $s_0(t)$ and $s_1(t)$, which are functions of time t, at $a = 0$ and $a = l$, respectively. To obtain the drawdown in the aquitard, the following initial and boundary conditions are needed.

$$s(a,0)=f(a)\quad 0<a<l\#(8)$$

$$s(0,t)=s_0(t)\qquad t>0\#(9)$$

$$s(l,t)=s_1(t)\qquad t>0\#(10)$$

2.2 Analytical Solutions

The solution to equations (7)-(10) can be derived by variable transformation and the characteristic function method. Details to the derivation of the mathematical model are listed in the Appendix. The drawdown variation in the aquitard is given as,

$$s(a,t)=\frac{\sigma_0'}{\gamma_w}\left(10^{w(a,t)}-1\right)\#(11)$$

Where：

$$w(a,t) = \sum_{n=1}^{\infty}\left[T_n(0)e^{-\frac{n^2\pi^2 c_v t}{l^2}} + e^{-\frac{n^2\pi^2 c_v t}{l^2}}\int_0^t f_n(t)e^{\frac{n^2\pi^2 c_v t}{l^2}}dt\right]\sin\frac{n\pi a}{l}$$

$$+ log_{10}\frac{\sigma_0' + \gamma_w s_0(t)}{\sigma_0'} + \frac{a}{l}log_{10}\frac{\sigma_0' + \gamma_w s_1(t)}{\sigma_0' + \gamma_w s_0(t)}$$

$$T_n(0) = \frac{2}{l}\int_0^l \log_{10}\frac{\sigma_0' + \gamma_w f(a)}{\sigma_0'}sin\frac{n\pi a}{l}da\sin\frac{n\pi a}{l}$$

$$+\frac{2}{n\pi}\left(\log_{10}\frac{\sigma_0' + \gamma_w s_1}{\sigma_0'}(-1)^n - \log_{10}\frac{\sigma_0' + \gamma_w s_0}{\sigma_0'}\right)$$

$$f_n(t) = \frac{2}{n\pi\ln 10}\left[\frac{(-1)^n\gamma_w}{\sigma_0' + \gamma_w s_1(t)}\frac{\partial s_1(t)}{\partial t} - \frac{\gamma_w}{\sigma_0' + \gamma_w s_0(t)}\frac{\partial s_0(t)}{\partial t}\right]$$

and s_0 and s_1 are the abrupt drawdown in the aquifers above and under the aquitard at the initial time, respectively.

According to Darcy's law, the flux per unit horizontal area at position a and at time t is given by $q(a,t) = k(\partial s/\partial a)$. According to the principle of water balance, the leakage rate of aquitard per unit horizontal area $q(t)$, which is equal to the $q(a,t)$ at location $a = l$ minus that at location $a = 0$ at time t can be expressed by equation (12).

$$q(t) = \frac{c_c c_v}{(1+e_0)l}\frac{\partial w}{\partial a}\#(12)$$

The hydraulic head of the pumped aquifer often varies both temporally and spatially (Neuman & Gardner, 1989). Sometimes, the drawdown may increase linearly with time (Zhuang et al., 2015). However, most regions lack data on drawdown history of pumped aquifers, especially in developing countries (Konikow & Neuzil, 2007) and during the early stage of groundwater exploitation (Shi et al., 2008) due to scarcity in monitoring technology to sustainably extract groundwater. In addition, the solution (equations (11) and (12)) includes terms of integration and derivation, which makes the calculation difficult.

Here, the temporal variations of drawdown history with sparse data were considered and the drawdown history was separated into many periods, each of which the drawdown is constant and is defined as $\varphi_{0,i}$ and $\varphi_{1,i}$ (i =1, 2…m) for the aquifers lying above and under the aquitard, respectively (Figure. 2). Namely, $s_0(t)$ and $s_1(t)$ were defined as a piecewise continuous step function (equation (13)). Meanwhile, to improve the accuracy of the estimation method, we quote the value of "Representative time" in each period of the drawdown history, "If the rate of drawdown is relatively stable over time, when the time of fixed drawdown is half that of linear drawdown, the water release from consolidation is basically the same" (Konikow & Neuzil, 2007). The history of the hydraulic head decline of adjacent aquifers and the step changes in hydraulic head for the analytical solutions are shown in Figure 2.

$$[s_0(t), s_1(t)] = \begin{cases} [\varphi_{0,1}, \varphi_{1,1}] & t_0 \leq t \leq t_1 \\ [\varphi_{0,2}, \varphi_{1,2}] & t_1 \leq t \leq t_2 \\ \cdots\cdots & \\ [\varphi_{0,m}, \varphi_{1,m}] & t_{m-1} \leq t \leq t_m \end{cases}, m \geq 1 \#(13)$$

Figure 2. Drawdown versus time defined as a step-by-step piecewise function.

The leakage rate of the aquitard per unit horizontal area (L^3T^{-1}) caused by variable drawdown in adjacent aquifers, which are step-by-step piecewise functions with respect to time, is obtained by substituting equation (13) into equation (12), given as,

$$q(\square) = \frac{C_c C_v}{(1 + e_0)l} \bar{q}(\square) \#(14)$$

where $\bar{t} = \frac{c_v t}{l^2}$,

$$\bar{q}(\bar{t}) = 2\sum_{i=0}^{m-1}\sum_{n=1}^{\infty}[(-1)^n - 1]\left((-1)^n \log_{10}\frac{\sigma'_{1,i+1}}{\sigma'_{1,i}} - \log_{10}\frac{\sigma'_{0,i+1}}{\sigma'_{0,i}}\right)e^{-n^2\pi^2(\bar{t}_m - \bar{t}_i)} ,$$

$\sigma'_{0,i} = \sigma'_0 + \gamma_w\varphi_{0i}$ and $\sigma'_{1,i} = \sigma'_0 + \gamma_w\varphi_{1i}$.

The cumulative water released from the aquitard per unit horizontal area $Q(\bar{t})$ (L^3) can be obtained through the integration of $q(\bar{t})$ over time.

$$Q(\bar{t}) = \int q(^{-})d\bar{t} = \frac{C_c l}{(1 + e_0)}\bar{Q}(\bar{t})\#(15)$$

where $\bar{Q}(\bar{t}) = 2\sum_{i=0}^{m-1} \sum_{n=1}^{\infty}\frac{[1-(-1)^n]}{n^2\pi^2}\left((-1)^n \log_{10}\frac{\sigma'_{1,i+1}}{\sigma'_{1,i}} - \log_{10}\frac{\sigma'_{0,i+1}}{\sigma'_{0,i}}\right)\left(1 - e^{-n^2\pi^2(\bar{t}_m - \bar{t}_i)}\right)$.

The above analytical method can be used to estimate the water release from the aquitard due to fluctuating hydraulic head in adjacent aquifers, especially lacking the drawdown history data during the early stage of groundwater exploitation. Compared with the solutions based on Terzaghi's theory (Li et al., 2017), the solution (equation 11) in this study considers the nonlinear change of compressibility and permeability during aquitard consolidation. Therefore, the proposed method is more practical and accurate for the purposes of estimating groundwater resources and the corresponding consolidation problem compared to traditional linear theory. In addition, we are interested in a relatively compressible aquitard and can ignore the compressibility of water and soil particles. Consequently, land subsidence caused by the depletion of groundwater stored in aquitard equals the value of Q. This method can be used to determine the hydrogeological parameters with data of aquitard deformation and drawdown in adjacent aquifers.

3. Testing and Verification of the Analytical Solution

3.1 Analytical Solution under Abrupt Drawdown in Adjacent Aquifers

In this case, it is assumed that the hydraulic head distribution in the aquitard is uniform at initial time, and the hydraulic head in the aquifer underlying the aquitard is constant, namely, $s(l,t) = \varphi$, and the drawdown in the aquifer overlying the aquitard is constant ($s(0,t) = 0$ or φ). Substituting these boundary and initial conditions into equation (15), the Q (L^3) of the aquitard undergoing drainage from one or both sides with constant drawdown are obtained respectively, as equation (16a) and (16b).

$$Q(\bar{t}) = \frac{2C_c l}{(1+e_0)} \log_{10}\left(\frac{\sigma_f^{'}}{\sigma_0^{'}}\right) \sum_{n=1}^{\infty} \frac{[1-(-1)^n]}{n^2\pi^2}\left(1-e^{-n^2\pi^2\bar{t}}\right) \#(16\text{a})$$

$$Q(\bar{t}) = \frac{4C_c l}{(1+e_0)} \log_{10}\left(\frac{\sigma_f^{'}}{\sigma_0^{'}}\right) \sum_{n=1}^{\infty} \frac{[1-(-1)^n]}{n^2\pi^2}\left(1-e^{-n^2\pi^2\bar{t}}\right) \#(16\text{b})$$

By comparing the Q of the aquitard undergoing drainage from one side (equation (16a)) with those of the aquitard undergoing drainage from both sides (equation (16b)), it can be found that the Q from the aquitard undergoing drainage from both sides is twice that of the aquitard undergoing drainage from one side, while the drawdown of aquifers on both sides of the aquitard is the same.

To determine the hydrogeological parameters of the aquitard, while the drawdown increases by φ in the adjacent aquifer, the logarithmic forms of equations (16a) and (16b) in a dimensionless form ($\bar{Q}$) and dimensionless time ($\bar{t}$) are respectively expressed as:

$$\log_{10}\overline{Q}(\bar{t}) = \log_{10} Q(t) + \log_{10}\left[\frac{(1+e_0)}{C_c l \log\left(\sigma_{\mathrm{f}}^{'}/\sigma_0^{'}\right)}\right] \#(17\text{a})$$

$$\log_{10}\bar{t} = \log_{10} t + \log_{10}\frac{c_v}{l^2} \#(17\text{b})$$

The type-curve approach is used to calculate the hydraulic parameters of the aquitard. Since the second term of the equation is a constant in the logarithmic plot, the data curve of the flux $Q(t)$ is analogous to the type-curve of the dimensionless deformation $\bar{Q}$. The method involves the following steps: 1) superimpose the $Q(t)$ curve on $\bar{Q}(\bar{t})$, while the axes of the two figures remain parallel; 2) Select any intersection of standard curve and $Q(t)$ test curve as the match point; and 3) then, the coordinates of the match points ($Q(t)$, $\bar{Q}(\bar{t})$, t and $\bar{t}$) are substituted into equations (18) and (19) to determine the parameters.

$$c_v = \frac{\bar{t}}{t} \cdot l^2 \#(18)$$

$$C_c = \frac{Q(t)(1+e_0)}{\log_{10}\left(\frac{\sigma_f'}{\sigma_0'}\right)\bar{Q}(\bar{t})l} \#(19)$$

3.2 Experimental test and Verification

To test the applicability of the formula and to verify the type-curve fitting method, the consolidated drainage data from Luo et al. (2020) are used in the study. A consolidation test of aquitard undergoing drainage from one side was carried out when the drawdown in the adjacent aquifer increases abruptly. The consolidation container is a cylinder with an inner diameter of 0.384 m, which is made of organic glass. The soil layer is divided into three layers from top to bottom: A middle silty clay layer with thickness of 0.24 m represented the aquitard. (l = 0.24 m), and its basic parameters are: e_0 = 0.869 and σ_0' = 2.77 kPa. The thicknesses of the upper and lower sand aquifers were 0.220 and 0.165 m. During the laboratory test, a constant decrease in hydraulic head of φ = 1 m was maintained, and the water depletion (Q) of the clay layer was recorded during the experiment.

The $Q(t)$ data curve and the type-curve of $\bar{Q}(\bar{t})$ are plotted in Figure 3, and superimposed by keeping the axes of the two graphs parallel to each other (Figure 3).

The coordinates of the match point are Q = 4.6×10^{-4}m^3, $\bar{Q}$ = 0.280, t = 2.8×10^3 s, and $\bar{t}$ = 0.076. The computed c_v and C_c are 1.56×10^{-6} m^2/s, 0.1496, respectively, by substituting these coordinates into equations (18) and (19). The specific storage S_s and k_v of the clay layer at the initial time are 0.125, 1.953×10^{-7} m/s calculated by $S_s = \frac{0.434\gamma_w C_c}{(1+e_0)\sigma_0'}$ and $k_v = \frac{0.434 c_v C_c \gamma_w}{(1+e_0)\sigma_0'}$, respectively. The hydraulic parameters determined in this study are basically equal to that calculated by Luo et al. (2020).

Figure 4 compares the measured depletion within the observation time of the clay layer and the results predicted by substituting these estimated parameters into the equation (16a) proposed in this study and the studies of Li et al. (2018) and Zhou et al. (2013). $Q(t)$ predicted by the analytical solution (7.15×10^{-4} m^3) in this study agrees well with the experimental results (7.11×10^{-4} m^3), and the $Q(t)$ predicted by the solutions in the studies of Li et al. (2018) and Zhou et al. (2013) are 1.03×10^{-3} and 1.71×10^{-3} m^3, respectively, which is larger than the measured deformation of the clay layer.

Figure 3. Determination of parameters by the type-curve fitting method.

Figure 4. Comparison of predicted and measured fluxes and settlement of the soil.

4. Evaluation and Discussion

4.1 Analytical Solutions under the Linear Drawdown in the Adjacent Aquifers

It is assumed that the hydraulic head distribution in the aquitard is uniform at initial time ($s(a, 0) = 0$), and the drawdown in the aquifers above and below the aquitard both increases linearly. Namely, the boundary conditions of the equation (7) are $s(0,t) = \beta_1 t$ and $s(l,t) = \beta_2 t$ (where β_1 and β_2 are the rate of drawdown in the aquifer overlying and underlying the aquitard, respectively) at the positions of a = 0 and a = l, respectively. Substituting these boundary conditions and initial condition into equation (12), the $q(t)$ of the aquitard undergoing drainage from both sides under the condition of linear drawdown is obtained,

$$q(t) = \frac{c_v C_c}{(1+e_0)l}\left\{\frac{2}{\ln 10}\sum_{\mathrm{n}=1}^{\infty}[(-1)^{\mathrm{n}}-1]\left[\mathrm{e}^{-\frac{\mathrm{n}^2\pi^2 c_v t}{l^2}}\int_0^t\left(\frac{(-1)^{\mathrm{n}}\gamma_w\beta_2}{\sigma_0'+\gamma_w\beta_2 t}-\frac{\gamma_w\beta_1}{\sigma_0'+\gamma_w\beta_1 t}\right)\mathrm{e}^{\frac{\mathrm{n}^2\pi^2 c_v t}{l^2}}dt\right]\right\} \#(20)$$

The $Q(t)$ of the aquitard undergoing drainage from both sides under the condition of linear drawdown is derived through integration of $q(t)$ over time.

$$Q(t) = \frac{c_v C_c}{(1+e_0)l}\frac{2}{\ln 10}\sum_{\mathrm{n}=1}^{\infty}[(-1)^{\mathrm{n}}-1]\int_0^t\left[\mathrm{e}^{-\frac{\mathrm{n}^2\pi^2 c_v t}{l^2}}\int_0^t\left(\frac{(-1)^{\mathrm{n}}\gamma_w\beta_2}{\sigma_0'+\gamma_w\beta_2 t}-\frac{\gamma_w\beta_1}{\sigma_0'+\gamma_w\beta_1 t}\right)\mathrm{e}^{\frac{\mathrm{n}^2\pi^2 c_v t}{l^2}}dt\right]dt \#(21)$$

4.2 Accuracy Evaluation

The proposed analytical method was tested and evaluated by application to a hypothetical system with specified hydraulic properties and boundary conditions. The $Q(t)$ of the aquitard undergoing drainage from both sides are twice that of the aquitard undergoing drainage from one side, while the drawdown of aquifers on both sides of the aquitard is the same. Here, we only analyze the water release of the aquitard undergoing drainage from one side shown as in Figure 1. Substantial groundwater withdrawal from wells in the underlying confined aquifer caused a linear increase in drawdown, which in turn induced depletion from the aquitard. According to the previous study (Li et al., 2019), the parameters used in this section are: C_c = 0.054, σ_0' = 51 kPa, e_0 = 1.10, c_v = 1.10×10^{-7} m/s^2, β = 1 m/year, and l = 10 m.

A comparison was made between the solutions of $Q(t)$ of the aquitard under the linear drawdown condition (equation (21)) and that estimated by the proposed analytical method (equation (15)) under the stepped drawdown condition. In order to evaluate the accuracy of the proposed method, we divided the drawdown history of the pumped aquifer into different numbers of periods to calculate the aquitard depletion. As shown in Figure 6, the $Q(t)$ predicted by equation (21) increases over time and it is 0.0473 m^3 at 10 years. The $Q(t)$ at 10 years predicted by equation (15) were 0.0492, 0.0480 and 0.0478 m^3, while the drawdown history of the pumped aquifer is divided into 1, 2 and 3 periods, respectively. The $Q(t)$ at 10 years as predicted by equation (15) is slightly greater than that predicted by equation (21), and the errors are about 4.02％, 1.47％ and 1.05％ for 1, 2 and 3 periods, respectively. Therefore, the accuracy of the proposed analytical method is very good for estimating groundwater depletion from the aquitard, and it is better while the period number of drawdown history increases.

Figure 5. The Cumulative amount of water released from the aquitard.

4.3 Parametric sensitivity for water release rate and depletion of aquitard

In order to investigate the effect of hydraulic parameters on the depletion from an aquitard under the condition of increasing drawdown, we conduct a parametric sensitivity analysis of the aquitard depletion, by varying the values in sections 4.2 at a time. This section analyzed the effect of the C_c, e_0, c_v, σ_0' l and β on water release rate and depletion of the aquitard undergoing drainage from one side. In addition, we compared the water release under the conditions of linear drawdown and fixed drawdown in the adjacent aquifer, and we take half of the total time as the “Representative time” while calculating the water depletion of the aquitard when the drawdown in the adjacent aquifer increases abruptly (Konikow & Neuzil, 2007).

Figure 6. The water release rate of the aquitard with the linear drawdown in the pumped aquifer for different values of (a) C_c (b) e_0, (c) c_v, (d) σ_0', (e) l and (f) β.

The $q(t)$ of the aquitard under the conditions of linear drawdown is predicted by equation (20) (see Figure 6). The $q(t)$ increases rapidly to a maximum initially, then it decreases, and the rate of decrease gradually slows down. The variation of $q(t)$ under different values of parameters also increases to a maximum initially, then it gradually decreases. Namely, the effect of the parameter values on $q(t)$ decreases under the condition of the linear drawdown over long timescales.

The $q(t)$ of the aquitard draining from one side are calculated with different C_c values (see Figure 6a). The $q(t)$ increases with increasing C_c, and the occurrence time for the maximum value of $q(t)$ does not depend on the value of C_c. The maximum values of $q(t)$ are 5.11×10^{-3}, 1.02×10^{-2}, 1.53×10^{-2}, 2.04×10^{-2} m^3/year, while the corresponding values of C_c are 0.05, 0.10, 0.15 and 0.20, respectively, and the occurrence time for the $q(t)$ maximum value is 4.2 years.

The $q(t)$ of the aquitard draining from one side are calculated with different e_0 values (see Figure 6b). The $q(t)$ decreases with increasing e_0, and the occurrence time for the maximum value of $q(t)$ does not depend on the value of e_0. The maximum values of $q(t)$ are 7.72×10^{-3}, 5.79×10^{-2}, 4.63×10^{-2}, 3.89×10^{-2} m^3/year, while the corresponding values of e_0 are 0.5, 1.0, 1.5 and 2.0, respectively, and the occurrence time for the $q(t)$ maximum value is 3.85 years.

The $q(t)$ of the aquitard draining from one side are calculated with different c_v values (see Figure 6c). The $q(t)$ is greater with a larger value of c_v at the initial stage, and then it is less with a larger value of c_v. The occurrence time for the maximum value of $q(t)$ decreases with an increasing c_v. The maximum values of $q(t)$ are 5.36×10^{-3}, 6.57×10^{-3}, 8.00×10^{-3}, 8.83×10^{-3} m^3/year, and the occurrence time for the $q(t)$ maximum values are 4.35, 2.85, 1.4 and 0.95 years, while the corresponding values of c_v are 1×10^{-7}, 2×10^{-7}, 5×10^{-7} and 1×10^{-6} m^2/s, respectively. The $q(t)$ are 1.03×10^{-3}, 9.99×10^{-4}, 9.83×10^{-4}, 9.78×10^{-4} m^3/year at the 50th year, while the corresponding values of c_v are 1×10^{-7}, 2×10^{-7}, 5×10^{-7} and 1×10^{-6} m^2/s, respectively.

The $q(t)$ of the aquitard draining from one side are calculated with different σ_0' values (see Figure 6d). The $q(t)$ decreases with an increasing σ_0', and the occurrence time for the maximum value of $q(t)$ increases with an increasing σ_0'. When the σ_0' values are 50, 100, 150 and 200 kPa, the maximum values of $q(t)$ are 1.46×10^{-2}, 9.99×10^{-3}, 5.53×10^{-3} and 3.42×10^{-3} m^3/year, and the occurrence time for $q(t)$ maximum values are 2.10, 2.75, 4.15, 5.25 years, respectively.

The $q(t)$ of the aquitard draining from one side are calculated with different l values(see Figure 6e). The $q(t)$ increases with an increasing l, and the occurrence time for the maximum value of $q(t)$ increases with an increasing l. When the values of l are 5, 10, 15 and 20 m, the maximum values of $q(t)$ are 3.91×10^{-3}, 5.50×10^{-3},

6.18×10^{-3}, 6.44×10^{-3} m^3/year, and the occurrence time for $q(t)$ maximum values are 1.75, 3.65, 6.45, 9.50 years, respectively.

The $q(t)$ of the aquitard draining from one side are calculated with different β values (see Figure 6f). The $q(t)$ increases with an increasing β, and the occurrence time for the maximum value of $q(t)$ decreases with an increasing β. While the values of β are 0.5, 1, 1.5 and 2 m/year, the maximum values of $q(t)$ are 3.06×10^{-3}, 5.36×10^{-3}, 6.57×10^{-3} and 7.86×10^{-3} m^3/year, and the occurrence time for $q(t)$ maximum values are 5.32, 4.45, 3.55 and 3.15 years, respectively.

Figure 7. Depletion of the aquitard with a linear drawdown in the pumped aquifer for different values of (a) l, (b) c_v, (c) σ'_0, and (d) β_1.

The depletion of the aquitard under the conditions of linear drawdown and constant drawdown, which are respectively predicted through equations (21) and (16a), increases with an increasing C_c (Figure 7a), and the difference of $Q(t)$ between the two cases increases with an increasing C_c. In particular, the estimated depletion of the aquitard under the linear drawdown conditions are 0.116, 0.231, 0.347, 0.463 m^3, and that under the constant drawdown conditions are 0.118, 0.236, 0.354, 0.472 m^3, which are 0.05, 0.10, 0.15 and 0.20, for corresponding values of C_c, respectively, and the error of the estimation method is 2.03%.

The $Q(t)$ of the aquitard draining from one side are calculated with different e_0 values (see Figure 7b). The $Q(t)$ predicted under the conditions of linear drawdown and constant drawdown decreases with an increasing e_0 and the difference of aquitard depletion between two cases decreases with an increasing value of e_0. In particular, the estimated depletion of the aquitard under the linear drawdown conditions are 0.175, 0.131, 0.105, 0.0874 m^3, and that under the constant drawdown condition are 0.179, 0.134, 0.107, 0.0875 m^3, which are 0.5, 1.0, 1.5 and 2.0, for corresponding values of e_0, respectively, and the error of the estimation method is 2.28％.

The $Q(t)$ of the aquitard draining from one side are calculated with different c_v values (see Figure 7c). The $Q(t)$ increases slightly with an increasing c_v under the conditions of linear drawdown and constant drawdown decreases and the final $Q(t)$ does not depend on c_v under the constant drawdown condition, while the consolidation rate accelerates with increasing c_v. In particular, the predicted depletion of the aquitard under the linear drawdown condition are 0.124, 0.126, 0.127 and 0.127 m^3, and that under the constant drawdown condition are 0.128 m^3, and the errors are 3.2％, 1.6％, 0.78％, 0.78％ corresponding values of c_v, which are 1×10^{-7}, 2×10^{-7}, 5×10^{-7} and 1×10^{-6} m^2/s, respectively.

The $Q(t)$ of the aquitard draining from one side are calculated with different σ_0' values (see Figure 7d). The $Q(t)$ predicted under the conditions of linear drawdown and constant drawdown decreases with an increasing σ_0' and the difference of aquitard depletion between the two cases increases with an increasing σ_0'. In particular, when the σ_0' values are 50, 100, 150 and 200 kPa, the estimated depletion of the aquitard under the linear drawdown condition are 0.125, 0.0933, 0.0764, 0.0649 m^3, and that under the constant drawdown condition are 0.128, 0.0960, 0.0787, 0.0672 m^3, and the errors are 2.4％, 2.9％, 3.0％ and 3.5％, respectively.

The $Q(t)$ of the aquitard draining from one side are calculated with different l values (see Figure 7e). The $Q(t)$ predicted under the conditions of linear drawdown and constant drawdown increases with an increasing l, and the difference of the $Q(t)$ between the two cases increases with an increasing value of l. In particular, when the values of l are 5, 10, 15 and 20 m, the predicted $Q(t)$ under the linear drawdown condition are 0.0636, 0.125, 0.182 and 0.229 m^3, and that under the constant drawdown condition are 0.0639, 0.128, 0.188 and 0.237 m^3, and the errors are 3.1%, 3.2%, 3.3%, and 3.5% for corresponding values of l, respectively.

The $Q(t)$ of the aquitard draining from one side are calculated with different β values (see Figure 7f). The $Q(t)$ predicted under the conditions of linear drawdown and constant drawdown decreases with an increasing β, and the difference of aquitard depletion between the two cases slightly decreases with an increasing β. When the values of β are 0.5, 1, 1.5 and 2 m/year, the estimated depletion of the aquitard under the linear drawdown condition are 0.0928, 0.125, 0.145 and 0.159 m^3, and that under the constant drawdown condition are 0.0953, 0.128, 0.148 and 0.162 m^3, and the errors are 2.8%, 2.1% 1.4% and 1.2%, , respectively.

5. Field application

5.1 Hydrogeologic Setting

The proposed method is also tested using data from a field site in Shanghai city, China. Shanghai is a large metropolis located in the east of China and occupies an area of nearly 6,340 km^2, (Figure 8). Shanghai City is underlain by a multi-layered aquifer system composed of Quaternary sediments, with an average of 280 m (Zhang et al., 2013). In 1860, Shanghai began to extract groundwater from deep wells, and land subsidence was first reported in 1921. The long-term over-exploitation of groundwater in aquifers has led to serious land subsidence (Shi et al., 2008; Zhang et al., 2007). The average total accumulated settlement in the city center was about 1.93 m, and the maximum was 2.63 m from 1921 to 2001 (Zhang et al., 2015).

To detect groundwater level changes and the compaction of individual strata, there are 27 extensometer groups and more than 1,400 observation wells in Shanghai (Figure 8) (Chai et al., 2004). The drawdown of hydraulic head in Shanghai can be divided into three stages. During the first stage, since the first observation of land subsidence in 1921, the continuous decline of groundwater level until 1965 led to a fast rate of land subsidence in Shanghai during this period, the net groundwater pumping rates and the average yearly rates of subsidence are 1.40×10^8 m^3/year and 32 mm/year. During the second stage, the pumping capacity decreased significantly from 1965 to 1981 to reduce the rate of land subsidence, and the average pumping capacity reached 0.38×10^8 m^3/year. Moreover, due to large-scale artificial recharge of groundwater being carried out in the central urban area, the annual land subsidence rate resulted in a negative growth to -3mm/year. During the third stage, due to rapid economic development, the amount of groundwater exploitation increased and the groundwater level decreased slowly after 1981, but it was still higher than the groundwater level in the 1960s. The net groundwater pumping rates and the average yearly rates of subsidence are 1.13×10^8 m^3/year and 8.2 mm/year until the reduction of groundwater extraction after 2001.

Here, extensometer group four, which has long-term observation data of the compaction of individual strata and variable drawdown, is taken as an example. There are three aquitards, one unconfined aquifer, and four confined aquifers at extensometer group four shown as in the stratigraphic distribution at the site of extensometer group four (Figure 9). The unconfined aquifer (UA) was composed of silty sand and buried from 0 m to 7 m below the ground surface, and could be recharged directly by surface water. Therefore, the annual average water level in UA has remained almost unchanged over years. The first confined aquifer (CA1) and the second confined aquifer (CA2), which are mainly composed of sand, were primarily pumped aquifers in this area and buried from 30 m to 48 m and 88 m to 153 m below the ground surface, respectively. The hydraulic head of the CA1 and CA2 dropped by 5.0 m, and the yearly decline rates of the hydraulic head both are about 0.25 m/year from 1981 to 2001. The total land subsidence during 1981–2001 was 226.48 mm, and the cumulative compaction of aquitard 1 and aquitard 2 was 55.25 and 22.84 mm, respectively, which is about 24.39% and 10.08% of the total subsidence during 1981–2001 (Figure 10) (Shi et al., 2008).

Figure 8. Location map and administrative divisions of Shanghai, and the locations of extensometer groups modified from Li et al. (2021).

Figure 9. Physical and mechanical properties of soil layers (modified from Zhang et al. (2007).

Figure 10. Groundwater level variations in confined aquifers, land subsidence, and compaction of individual strata at extensometer group four modified from Zhang et al. (2007).

5.2 Determination of Aquitard Parameters

Due to the lack of specific compression distribution of each layer, the aquitard is simplified as a homogeneous confining layer for analysis and treatment to determine the overall average hydrogeological parameters over the whole thickness. The water level of UA has remained almost unchanged over the period of 1981 – 2001, thus it is inferred that the deformation of aquitard 1 was caused by the drawdown in CA1. Meanwhile, the deformation of aquitard 2 was inferred to be caused by the drawdown in CA1 and CA2. Therefore, aquitards 1 and 2 are regarded as the aquitard undergoing drainage from one and both sides, respectively.

In order to determine the hydrogeological parameters of aquitards 1 and 2, we only consider the drawdown history from 1981 to 2001 and divide 20 years of drawdown history into 3 periods, each being Δt to be 6.67 years. Thus, we have constant drawdowns during the 3 periods to be 1.6, 1.6, and 1.8 m, respectively, leading to φ_1^1 = 1.6 m, φ_2^1 = 1.6 m, and φ_3^1 = 1.8 m, where the superscript 1 represents aquitard 1. For aquitard 2, the stepped drawdown during the 3 periods in CA1 and CA2 are: $\varphi_{0,1}^2 = \varphi_{1,1}^2 =$ 1.6 m, $\varphi_{0,2}^2 = \varphi_{1,2}^2 =$ 1.6 m, and $\varphi_{0,3}^2 = \varphi_{1,3}^2 =$ 1.8 m, respectively. In addition, parameters of the aquitard 1 and aquitard 2 are as follow: l^1 = 23 m, e_0^1 = 1.10, $\sigma_0^{1\prime}$ = 150 kPa, l^2 = 40 m, e_0^2 = 0.93, and $\sigma_0^{2\prime}$ = 610 kPa.

Similar to section 3.1, the type-curve fitting method determines the hydrogeological parameters of the aquitard. The logarithmic forms of equation (15) in a dimensionless form ($\bar{Q}(\bar{t})$) and dimensionless time ($\Delta\bar{t} = \frac{c_v \Delta t}{l^2}$) are respectively expressed as:

$$\log_{10} \bar{Q}(\bar{t}) = \log_{10} Q(t) + \log_{10} \left[\frac{1 + e_0}{C_c l}\right] \#(22a)$$

$$\log_{10} \Delta\bar{t} = \log_{10} \Delta t + \log_{10} \frac{c_v}{l^2} \#(22b)$$

Because the value of c_v affects the dimensionless time ($\Delta\bar{t}$), we plotted the type curve under different $\Delta\bar{t}$ values and fitted the measured data with a type curve to determine the c_v value. The type curve of $\bar{Q}(\bar{t})$ under different $\Delta\bar{t}$ values is presented in Figure 11. In addition, we keep the final point of the measured data to coincide with the final point of the dimensionless curve, while superimposing $Q(t)$ curve over $\bar{Q}(\bar{t})$, and selecting the matching point as the intersection of the type curve and the $Q(t)$ data curve. Then, substitute the coordinates of the match points $Q(t)$、 $\bar{Q}(\bar{t})$、 Δt and $\Delta\bar{t}$ into equations (26) and (27) to determine the hydrogeological parameters.

$$c_v = \frac{l^2 \Delta\bar{t}}{\Delta t} \#(23)$$

$$C_c = \frac{Q(t)(1 + e_0)}{\bar{Q}(\bar{t}) l} \#(24)$$

The measured values of $Q(t)$ of aquitard 1 match the type-cure $\bar{Q}(\bar{t})$ of $\Delta\bar{t}$ is 0.30, and its coordinates in the two systems are Q = 2.6×10^{-2} m^3, $\bar{Q}$ = 3.2×10^{-2}, t = 12 years and $\bar{t}$ = 0.46 (see Figure 9a). Substituting these values into equations (23) and (24) yields the estimated coefficient of consolidation, c_{v1} =7.62×10^{-7} m^2/s, and the compression index, c_{c1} =0.074, of aquitard 1. The S_s and k_v of the aquitard 1 at initial time respectively are 9.9×10^{-4} m^{-1} and 7.62×10^{-10} m/s, which can be calculated by

$S_s = \frac{0.434\gamma_w C_c}{(1+e_0)\sigma_0'}$ and $k_v = \frac{0.434 c_v C_c \gamma_w}{(1+e_0)\sigma_0'}$, respectively.

The measured values of $Q(t)$ of aquitard 2 match the type-curve $\bar{Q}(\bar{t})$ of $\Delta\bar{t}$ is 0.10, and its coordinates in the two systems are Q = 1.26×10^{-2} m^3, $\bar{Q}$ = 9.8×10^{-2}, t = 13 years and $\bar{t}$ = 0.18 (see Figure 9b). The estimated coefficient of consolidation, c_{v2} =7.57×10^{-7} m^2/s, and the compression index, C_{c2} = 0.063, of aquitard 2. The S_s and k_v of the aquitard 2 at an initial time are 2.3×10^{-4} m^{-1} and 1.75×10^{-10} m/s, respectively.

Figure 11. Determination of parameters by the type-curve fitting method: (a) aquitard 1; (b) aquitard 2.

5.3 Verification and Discussion

The above estimated hydrogeological parameters are substituted into the equation (21) to obtain the estimated $Q(t)$ of aquitard 1 and aquitard 2 under the condition of linear drawdown. Figure 12 shows the estimated and measured curves of the $Q(t)$. In particular, the estimated and measured depletion of the aquitard 1 per unit horizontal area respectively are 0.054 and 0.055 m^3, while the corresponding error value is 1.8%. The estimated and measured depletion of the aquitard 2 per unit horizontal area respectively are 0.023 and 0.022 m^3, while the corresponding error is 4.3%. It is seen that the depletion of the aquitard predicted by the analytical solution in this study agrees well with the measured results, which means the accuracy of the hydrogeological parameters determined by the proposed method.

Figure 12. Comparison of predicted and measured settlement of the aquitard 1 and 2.

The values of k_v and S_s, in fact, decrease with the increasing effective stress with the development of consolidation of the aquitard. The estimated k_v and S_s at the lower surface of aquitard 1 in 2001 were 5.71×10^{-10} m/s and 7.4×10^{-4} m^{-1}, respectively. Similarly, the estimated k_v and S_s at the lower surface of aquitard 2 in 2001 were 1.69×10^{-10} m/s and 2.22×10^{-4} m^{-1}, respectively.

By comparing the estimated and measured k_v and S_s with the results of the geologic method calibrated by Konikow & Neuzil (2007) (see Figure 13), the estimated and measured k_v were close to the clay layer with medium content, which is similar to the characteristics of clay in Shanghai (Zhang et al., 2007). It is found that the k_v and S_s of aquitards 1 and 2 are less than laboratory experimental results (Figure 9), due to the fact that both aquitards have experienced consolidation over a very long time and under originally extremely high-stress conditions, while the laboratory samples were inevitably subjected to stress perturbation due to many factors such as sample collection, transportation and laboratory installation (Konikow & Neuzil, 2007; Zhuang et al., 2015). The estimated S_s is closer to the soil parameters of over-consolidated soil, which is because the aquitards have undergone consolidation under greater effective stress caused by drawdown in the CA1 and CA2 before 1965.

Figure 13. Comparison of predicted and measured hydraulic conductivity (a) and specific storage (b) of the aquitard in the geologic method calibrated from Konikow & Neuzil (2007).

6. Conclusions

In this study, the hydrogeological conceptual model of a multi-layer aquifer system is constructed. Based on the theories developed by Davis & Raymond (1965) and Gibson et al. (1967), the governing equation for nonlinear consolidation of an aquitard is developed without considering the creep effect. A general analytical solution under nonhomogeneous initial conditions and arbitrary boundary conditions is proposed to describe the variation of drawdown in the aquitard undergoing nonlinear consolidation. Based on the analytical solution, methods to calculate the hydrogeological parameters and long-term decreases in the volume of water stored in the low permeability aquitard undergoing nonlinear consolidation are put forward, under a condition that the drawdown history of the aquifers above and underlying the aquitard can be approximated as step-by-step piecewise function with respect to time. In addition, factors affecting the $Q(t)$ are also studied under the conditions of constant and linearly increasing drawdown in the adjacent confined aquifer. The new method proposed in this study is demonstrated by a laboratory experiment and a field application to the aquifer system beneath Shanghai city of China. The main conclusions are as follows:

(1) Under the condition of linear drawdown in adjacent aquifers, the depletion of the aquitard increases with increasing C_c, β, l, c_v and it decreases with increasing e_0, σ_0', while it becomes independent of c_v over long timescales. The $q(t)$ of the aquitard increases initially and then it gradually decreases. The effect of the parameter values on the $q(t)$ tends to disappear over long timescales. The maximum value of the water release rate increases with increasing C_c, φ, l, c_v and decreasing e_0, σ_0'. The

occurrence time for the maximum value of $q(t)$ increases with increasing σ_0', l and decreasing c_v, β and it does not depend on the value of C_c and e_0.

(2) The proposed analytical method for calculating groundwater depletion of aquitard, of which the error is generally less than 4%, is very good, and its accuracy is better while the drawdown history of pumped aquifers is divided into more periods for estimation. By comparing groundwater depletion of aquitard under the conditions of linear drawdown and constant drawdown using "Representative time", the results are in good agreement, while the latter is slightly greater than the former.

(3) The estimated hydraulic parameters of the aquitards 1 and 2 at the selected field site are closer to the data of the soil layer with moderate clay content and over-consolidation, which is similar to the characteristics of clay found in Shanghai City, and they are in general agreement with the results of the geologic method developed by Konikow & Neuzil (2007). However, they are usually smaller than the experimental results due to long-term consolidation and stress disturbance during the test.

Acknowledgments

This study was financed by the Open Fund of State Key Laboratory of Geohazard Prevention and Geoenvironment Protection (Chengdu University of Technology) (SKLGP2021K023), the National Natural Science Foundation of China (41702253), and the China Scholarship Council for working at the University of Waterloo as a visiting scholar. Walter A. Illman appreciates the support of the Discovery Grant from the National Science and Engineering Research Council of Canada (NSERC), which

made this collaboration possible.

Data Availability Statement

The test data in the section 3.1-3.2 is available through Luo et al. (2020). Data, the parameter values in sections 4.1-4.3 is available through Li et al. (2019). Data, the parameter values in sections 5.1-5.3, is available through Zhang et al. (2007) and Konikow & Neuzil (2007).

Appendix: Derivation of Equation (11)

The mathematical statement of the problem consisting of equations (7) – (10) are as follows:

$$c_v\left[\frac{\partial^2 s}{\partial a^2}-\frac{\gamma_w}{\sigma_0'+\gamma_w s}\left(\frac{\partial s}{\partial a}\right)^2\right]=\frac{\partial s}{\partial t}\#(7)$$

$$s(a,0)=f(a)=0<a<l\#(8)$$

$$s(0,t)=s_0(t)\qquad t>0\#(9)$$

$$s(l,t)=s_1(t)\qquad t>0\#(10)$$

Using the substitution:

$$w=\log_{10}(\sigma'/\sigma_0')=\log_{10}((\sigma_0'+\gamma_w s)/\sigma_0')\qquad\text{(A1)}$$

The boundary conditions are simplified by substituting equation (A1) into equations (7) – (10) as follows:

$$c_v\frac{\partial^2 w}{\partial a^2}=\frac{\partial w}{\partial t}\#(\text{A2})$$

$$w(a,0)=\log_{10}\frac{\sigma_0'+\gamma_w f(a)}{\sigma_0'}\qquad 0<a<l\#(\text{A3})$$

$$w(0,t)=\log_{10}\frac{\sigma_0'+\gamma_w s_1(t)}{\sigma_0'}\qquad t>0\#(\text{A4})$$

$$w(l,t)=\log_{10}\frac{\sigma_0'+\gamma_w s_2(t)}{\sigma_0'}\qquad t>0\#(\text{A5})$$

Because boundary condition (A5) is non-homogeneous, it is necessary to simplify the boundary conditions as follows:

$$w(a,t) = p(a,t) + q(a,t) \tag{A6}$$

$$q(a,t) = \log_{10}\frac{\sigma_0' + \gamma_w s_1(t)}{\sigma_0'} + \frac{a}{l}\log_{10}\frac{\sigma_0' + \gamma_w s_2(t)}{\sigma_0' + \gamma_w s_1(t)} \tag{A7}$$

Substituting $w(a,t)$ with $p(a,t)$ of equation (A2), the initial condition and boundary condition leads to:

$$c_v\frac{\partial^2 p}{\partial a^2} - \frac{1}{\ln 10}\left(\frac{\gamma_w}{\sigma_0' + \gamma_w s_1(t)}\frac{\partial s_1(t)}{\partial t}\left(1 - \frac{a}{l}\right) + \frac{\gamma_w}{\sigma_0' + \gamma_w s_2(t)}\frac{\partial s_2(t)}{\partial t}\frac{a}{l}\right) = \frac{\partial p}{\partial t} \tag{A8}$$

$$p(a,0) = \log_{10}\frac{\sigma_0' + \gamma_w f(a)}{\sigma_0'} - \log_{10}\frac{\sigma_0' + \gamma_w s_1}{\sigma_0'} - \frac{a}{l}\log_{10}\frac{\sigma_0' + \gamma_w s_2}{\sigma_0' + \gamma_w s_1} \quad 0 < a < l \tag{A9}$$

$$p(0,t) = 0 \quad 0 < a < l \tag{A10}$$

$$p(l,t) = 0 \quad 0 < a < l \tag{A11}$$

where s_1, s_2 are the drawdown in the aquifers lying respectively above and below the aquitard at the initial time (*t*=0), respectively.

The solution of equations (A8) – (A11) was derived using the separation of variables method as:

$$p(a,t) = \sum_{n=1}^{\infty}[T_n(0)e^{-\frac{n^2\pi^2 c_v t}{l^2}} + e^{-\frac{n^2\pi^2 c_v t}{l^2}}\int_0^t f_n(t)e^{\frac{n^2\pi^2 c_v t}{l^2}}dt]\,sin\frac{n\pi a}{l} \tag{A12}$$

where

$$f_n(t) = \frac{2}{n\pi \ln 10}\left[\frac{(-1)^n\gamma_w}{\sigma_0' + \gamma_w s_2(t)}\frac{\partial s_2(t)}{\partial t} - \frac{\gamma_w}{\sigma_0' + \gamma_w s_1(t)}\frac{\partial s_1(t)}{\partial t}\right] \tag{A13}$$

$$T_n(0) = \frac{2}{l}\int_0^l \log_{10}\frac{\sigma_0' + \gamma_w f(a)}{\sigma_0'}\,sin\frac{n\pi a}{l}da + \frac{2}{n\pi}\left(\log_{10}\frac{\sigma_0' + \gamma_w s_2}{\sigma_0'}(-1)^n - \log_{10}\frac{\sigma_0' + \gamma_w s_1}{\sigma_0'}\right) \tag{A14}$$

Combining (A7) with (A12) to obtain the solution of equations (A2) – (A5) leads to,

$$w(a,t) = \sum_{n=1}^{\infty}\left[T_n(0)e^{-\frac{n^2\pi^2 c_v t}{l^2}} + e^{-\frac{n^2\pi^2 c_v t}{l^2}}\int_0^t f_n(t)e^{\frac{n^2\pi^2 c_v t}{l^2}}dt\right]sin\frac{n\pi a}{l} + \log_{10}\frac{\sigma_0' + \gamma_w s_1(t)}{\sigma_0'} + \frac{a}{l}\log_{10}\frac{\sigma_0' + \gamma_w s_2(t)}{\sigma_0' + \gamma_w s_1(t)} \tag{A15}$$

The solution of equation (11) was derived by substituting equation (A15) into equation (A1).

References

Arabameri, A., Saha, S., Roy, J., Tiefenbacher, J. P., Cerda, A., Biggs, T., Pradhan, B., Thi Ngo, P. T. & Collins, A. L. (2020). A novel ensemble computational intelligence approach for the spatial prediction of land subsidence susceptibility. *Science of the Total Environment* 726(C), 637-653. https://doi.org/10.1016/j.scitotenv.2020.138595

Bakr, M. (2015). Influence of Groundwater Management on Land Subsidence in Deltas:A Case Study of Jakarta (Indonesia). *Water Resources Management* 29(5), 1541-1555. https://doi.org/10.1007/s11269-014-0893-7

Burbey, T. J. (2003). Use of time–subsidence data during pumping to characterize specific storage and hydraulic conductivity of semi-confining units. *Journal of Hydrology* 281(1), 3-22. https://doi.org/10.1016/S0022-1694(03)00197-5

Burbey, T. J. (2020). Parameter estimation of a multiple aquifer-aquitard system from a single extensometer record: Las Vegas, Nevada, USA. *Proceedings of the International Association of Hydrological Sciences* 382, 51-56. https://doi.org/10.5194/piahs-382-51-2020

Chai, J., Shen, S., Zhu, H. & Zhang, X. (2004). Land subsidence due to groundwater drawdown in Shanghai. *Géotechnique* 54(2), 143-147. https://doi.org/10.1680/geot.2004.54.2.143

Custodio, E. (2002). Aquifer overexploitation: what does it mean? *Hydrogeology journal* 10(2), 254-277. https://doi.org/10.1007/s10040-002-0188-6

Davis, E. H. & Raymond, G. P. (1965). A Non-Linear Theory of Consolidation. *Géotechnique* 15(2), 161-173. https://doi.org/10.1680/geot.1965.15.2.161

Gibson, R. E., England, G. L. & Hussey, M. J. L. (1967). The Theory of One-Dimensional Consolidation of Saturated Clays. *Géotechnique* 17(3), 261-273. https://doi.org/10.1680/geot.1967.17.3.261

Gibson, R. E., Schiffman, R. L. & Cargill, K. W. (1981). The theory of one-dimensional consolidation of saturated clays. II. Finite nonlinear consolidation of thick homogeneous layers. *Canadian Geotechnical Journal* 18(2), 143-144. https://doi.org/10.1139/t81-030

Guo, Q. & Li, H. (2015). Terrestrial-originated submarine groundwater discharge through deep multilayered aquifer systems beneath the seafloor. *Hydrological Processes* 29(2), 295-309. https://doi.org/10.1002/hyp.10163

Konikow, L. F. & Kendy, E. (2005). Groundwater depletion: A global problem. *Hydrogeology Journal* 13(1), 317-320. https://doi.org/10.1007/s10040-004-0411-8

Konikow, L. F. & Neuzil, C. E. (2007). A method to estimate groundwater depletion from confining layers. *Water Resources Research* 43(7). https://doi.org/10.1029/2006WR005597

Li, M., Chen, J., Xu, Y., Tong, D., Cao, W. & Shi, Y. (2021). Effects of groundwater exploitation and recharge on land subsidence and infrastructure settlement patterns in Shanghai. *Engineering Geology* 282. https://doi.org/10.1016/j.enggeo.2021.105995

Li, Z. & Zhou, Z. (2015). An analytical solution for leakage rate and depletion of aquitard influenced by the delayed yield phenomenon. *Environmental Earth Sciences* 74(2), 1227-1234. https://doi.org/10.1007/s12665-015-4114-3

Li, Z., Zhou, Z., Chen, Z., Liu, G. & Zhou, C. (2017). An analytical method to estimate groundwater depletion from a confining layer. *Natural Hazards* 85(2), 887-906. https://doi.org/10.1007/s11069-016-2609-1

Li, Z., Zhou, Z., Dai, Y. & Dai, B. (2019). Contaminant transport in a largely-deformed aquitard affected by delayed drainage. *Journal of Contaminant Hydrology* 221, 118-126. https://doi.org/10.1016/j.jconhyd.2019.02.002

Li, Z., Zhou, Z., Li, M., Zhang, B., Dai, B. & Bai, Q. (2018). Delayed Drainage of a Largely Deformed Aquitard due to Abrupt Water Head Decline in Adjacent Aquifer. *Geofluids* 2018. https://doi.org/10.1155/2018/2326491

Liu, C., Shi, B., Gu, K., Zhang, T., Tang, C., Wang, Y. & Liu, S. (2022). Negative Pore Water Pressure in Aquitard Enhances Land Subsidence: Field, Laboratory, and Numerical Evidence. *Water Resources Research* 58(1), e2021WR030085. https://doi.org/10.1029/2021WR030085

Luo, H., Li, Z., Luo, M., Zhang, Q. & Illman, W. A. (2020). An analytical method to calculate groundwater released from an aquitard undergoing nonlinear consolidation. *Water Resources Research* 56(9). https://doi.org/10.1029/2020wr027320

Neuman, S. P. & Gardner, D. A. (1989). Determination of Aquitard/Aquiclude Hydraulic Properties from Arbitrary Water-Level Fluctuations by Deconvolution. *Groundwater* 27(1), 66-76. https://doi.org/10.1111/j.1745-6584.1989.tb00009.x

Neuman, S. P. & Witherspoon, P. A. (1969). Applicability of Current Theories of Flow in Leaky Aquifers. *Water Resources Research* 5(4), 817-829. https://doi.org/10.1029/WR005i004p00817

Shi, X., Wu, J., Xue, Y., Zhang, Y., Wei, Z. & Yu, J. (2007). The development and control of the land subsidence in the Yangtze Delta, China. *Environmental Geology* 55(8), 1725-1735. https://doi.org/10.1007/s00254-007-1123-x

Shi, X., Xue, Y., Wu, J., Ye, S., Zhang, Y., Wei, Z. & Yu, J. (2008). Characterization of regional land subsidence in Yangtze Delta, China: the example of Su-Xi-Chang area and the city of Shanghai. *Hydrogeology Journal* 16(3), 593-607. https://doi.org/10.1007/s10040-007-0237-2

Terzaghi, K. (1943) *Theoretical Soil Mechanics*, New York: Wiley.

Xie, K. & Leo, C. J. (2004). Analytical solutions of one-dimensional large strain consolidation of saturated and homogeneous clays. *Computers and Geotechnics* 31(4), 301-314. https://doi.org/10.1016/j.compgeo.2004.02.006

Ye, S., Xue, Y., Wu, J., Yan, X. & Yu, J. (2016). Progression and mitigation of land subsidence in China. *Hydrogeology Journal* 24(3), 685-693. https://doi.org/10.1007/s10040-015-1356-9

Zhang, X., Wang, J., Wong, H., Leo, C., Liu, Q., Tang, Y., Yan, X., Sun, W., Huang, Z. & Hao, X. (2013). Land subsidence caused by internal soil erosion owing to pumping confined aquifer groundwater during the deep foundation construction in Shanghai. *Natural Hazards* 69(1), 473-489. https://doi.org/10.1007/s11069-013-0718-7

Zhang, Y., He, G., Wu, J., Zhu, Z., Yan, X. & Yang, T. (2020a). Experimental study on mechanism for pumping-induced land subsidence. *Proceedings of the International Association of Hydrological Sciences* 382, 387-390. https://doi.org/10.5194/piahs-382-387-202

Zhang, Y., Wu, J., Xue, Y., Wang, Z., Yao, Y., Yan, X. & Wang, H. (2015). Land subsidence and uplift due to long-term groundwater extraction and artificial recharge in Shanghai, China. *Hydrogeology Journal* 23(8), 1851-1866. https://doi.org/10.1007/s10040-015-1302-x

Zhang, Y., Xue, Y. & Wu, J. (2007). Stress-Strain Measurements of Deforming Aquifer Systems that Underlie Shanghai, China. *Environmental & Engineering Geoscience* 13(3), 218-228. https://doi.org/10.2113/gseegeosci.13.3.217

Zhang, Y., Yan, X., Yang, T., Wu, J. & Wu, J. (2020b). Three-Dimensional Numerical Investigation of

Pore Water Pressure and Deformation of Pumped Aquifer Systems. *Ground water* 58(2), 278-290. https://doi.org/10.5194/piahs-382-387-2020

Zhao, Z., Illman, W. A., Zha, Y., Yeh, T. C. J., Mok, C. M. B., Berg, S. J. & Han, D. (2019). Transient Hydraulic Tomography Analysis of Fourteen Pumping Tests at a Highly Heterogeneous Multiple Aquifer–Aquitard System. *Water* 11(9). https://doi.org/10.3390/w11091864

Zhou, Z., Guo, Q. & Dou, Z. (2013). Delayed drainage of aquitard in response to sudden change in groundwater level in adjacent confined aquifer: Analytical and experimental studies. *Chinese Science Bulletin* 58(25), 3060-3069. https://doi.org/10.1007/s11434-013-5730-5

Zhuang, C., Zhou, Z., Zhan, H. & Wang, G. (2015). A new type curve method for estimating aquitard hydraulic parameters in a multi-layered aquifer system. *Journal of Hydrology* 527, 212-220. https://doi.org/10.1016/j.jhydrol.2015.04.062

Figure 1.

Unconfined or confined aquifer
$s(0, t) = s_0(t)$
0
l
Aquitard (C_c, e_0, C_v, σ'_0)
$s(a, 0) = f(a)$
Confined aquifer
$s(l, t) = s_1(t)$
a

Figure 2.

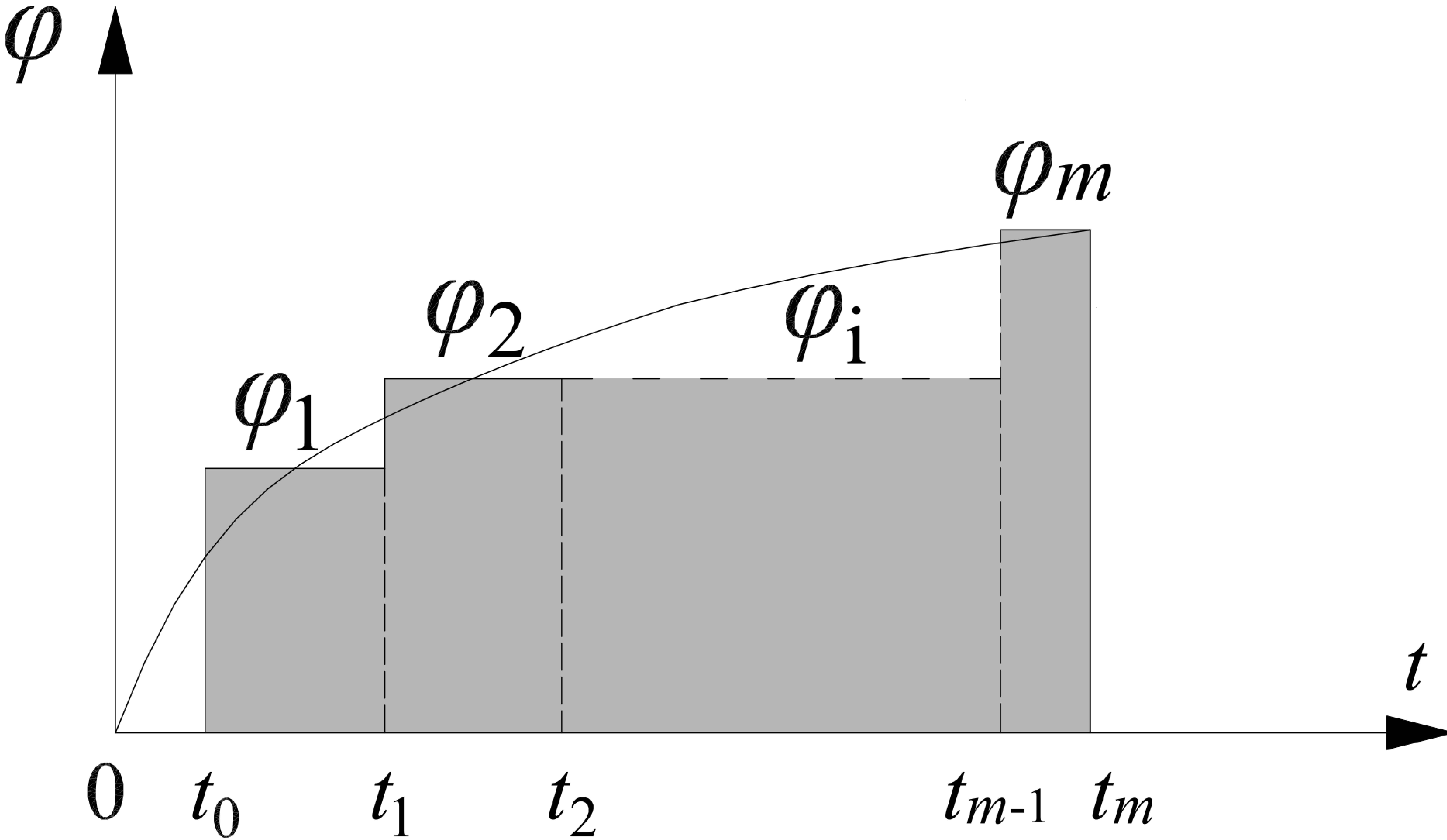

φ
φ_m
φ_2
φ_i
φ_1
t
0
t_0
t_1
t_2
t_{m-1}
t_m

Figure 3.

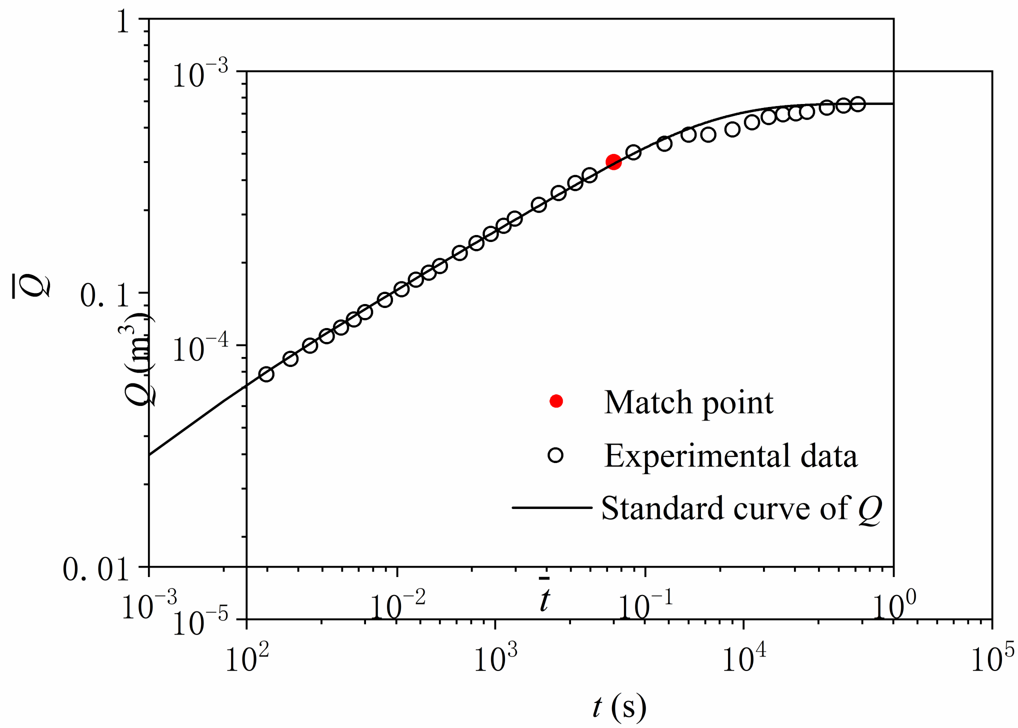

1
0. 1
0. 01
$\overline{Q}$
10^{-3}
10^{-4}
10^{-5}
Q (m^3)
10^{-3}
10^{-2}
$\bar{t}$
10^{-1}
10^{0}
10^{2}
10^{3}
10^{4}
10^{5}
t (s)
Match point
Experimental data
Standard curve of Q

Figure 4.

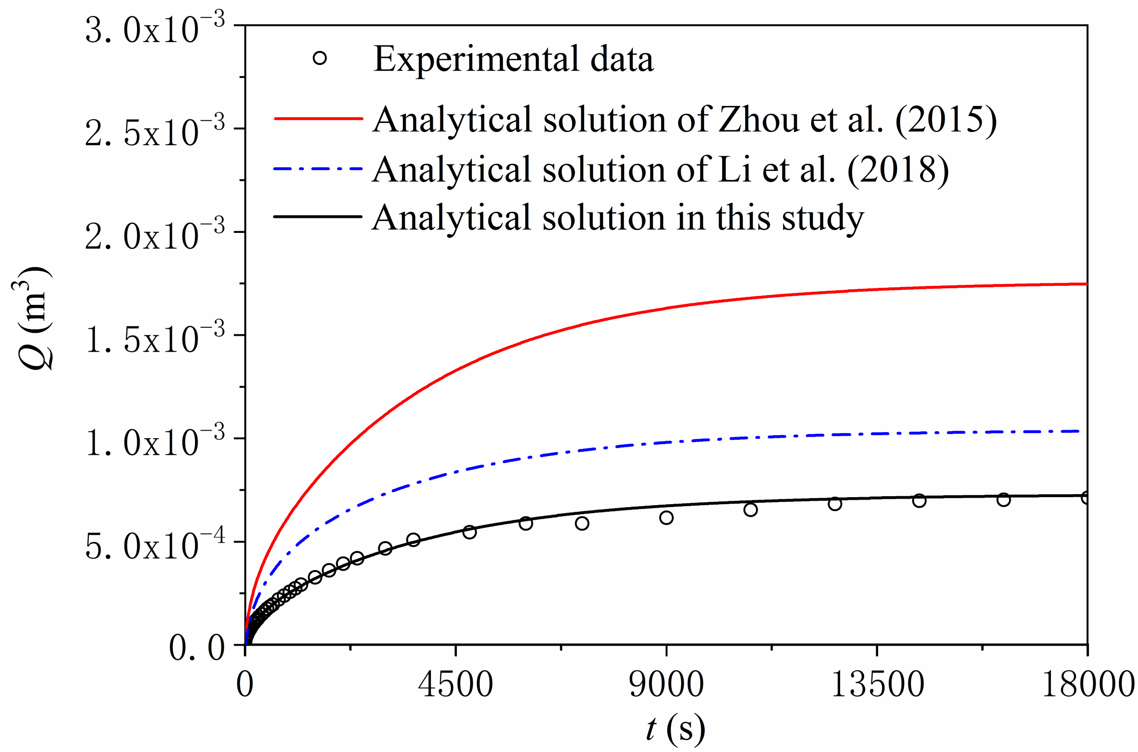

3. 0x10−3
2. 5x10−3
2. 0x10−3
1. 5x10−3
1. 0x10−3
5. 0x10−4
0. 0
Q (m3)
0
4500
9000
13500
18000
t (s)
Experimental data
Analytical solution of Zhou et al. (2015)
Analytical solution of Li et al. (2018)
Analytical solution in this study

Figure 5.

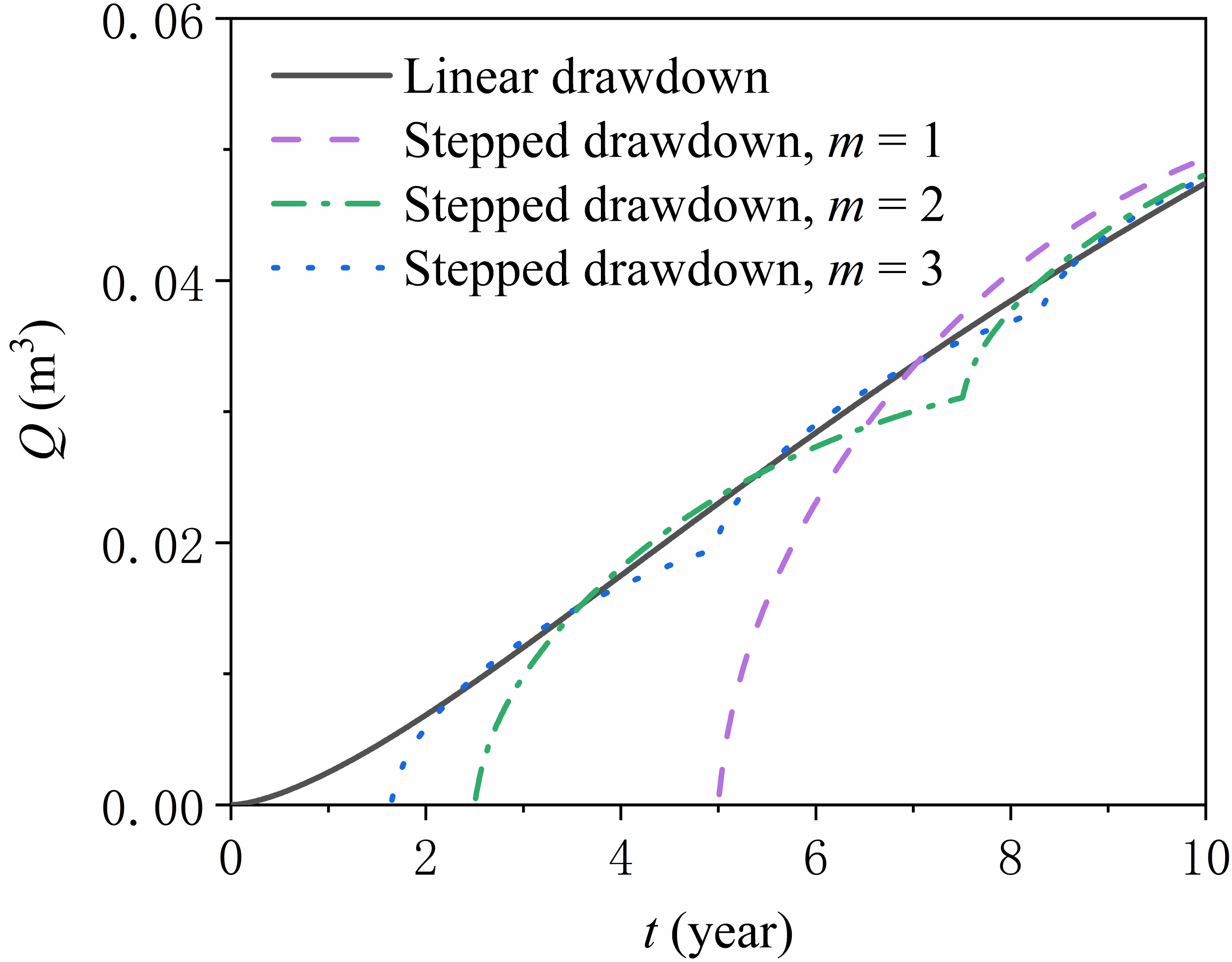

0. 06
0. 04
0. 02
0. 00
Q (m³)
0
2
4
6
8
10
t (year)
Linear drawdown
Stepped drawdown, m = 1
Stepped drawdown, m = 2
Stepped drawdown, m = 3

Figure 6.

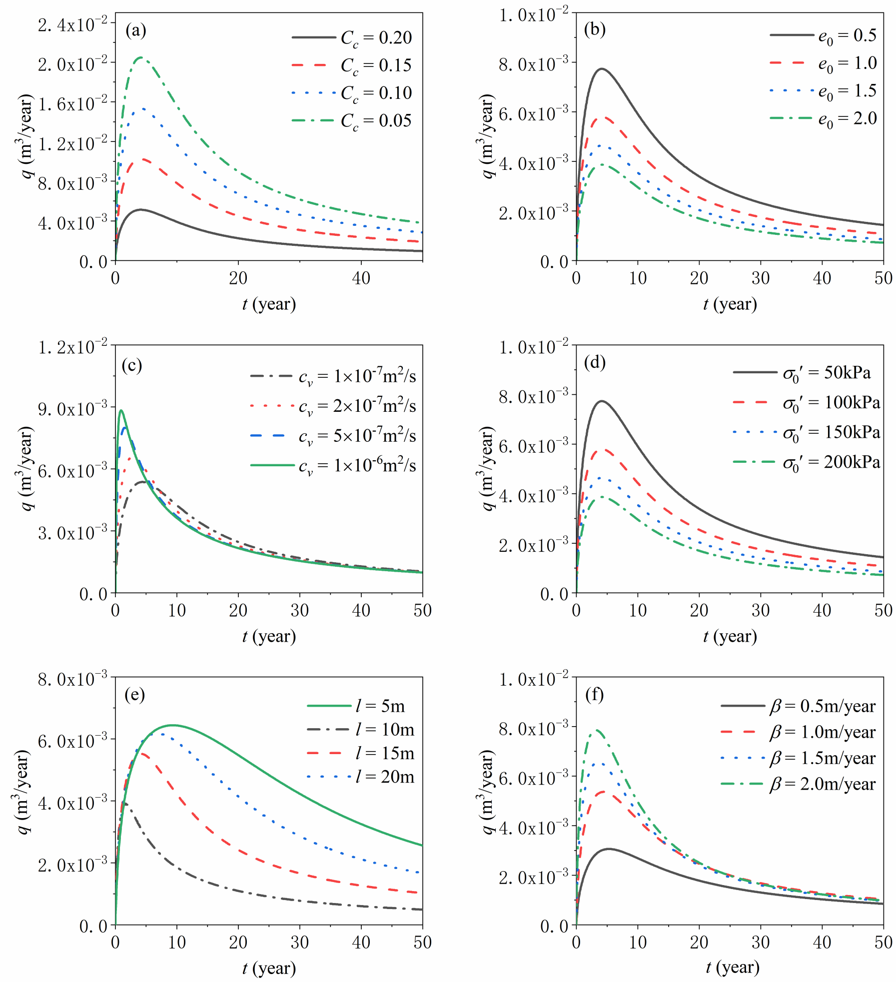
(a)
$C_c = 0.20$
$C_c = 0.15$
$C_c = 0.10$
$C_c = 0.05$
q (m^3/year)
t (year)
(b)
$e_0 = 0.5$
$e_0 = 1.0$
$e_0 = 1.5$
$e_0 = 2.0$
q (m^3/year)
t (year)
(c)
$c_v = 1\times10^{-7}$m^2/s
$c_v = 2\times10^{-7}$m^2/s
$c_v = 5\times10^{-7}$m^2/s
$c_v = 1\times10^{-6}$m^2/s
q (m^3/year)
t (year)
(d)
$\sigma_0' = 50$kPa
$\sigma_0' = 100$kPa
$\sigma_0' = 150$kPa
$\sigma_0' = 200$kPa
q (m^3/year)
t (year)
(e)
$l = 5$m
$l = 10$m
$l = 15$m
$l = 20$m
q (m^3/year)
t (year)
(f)
$\beta = 0.5$m/year
$\beta = 1.0$m/year
$\beta = 1.5$m/year
$\beta = 2.0$m/year
q (m^3/year)
t (year)

Figure 7.

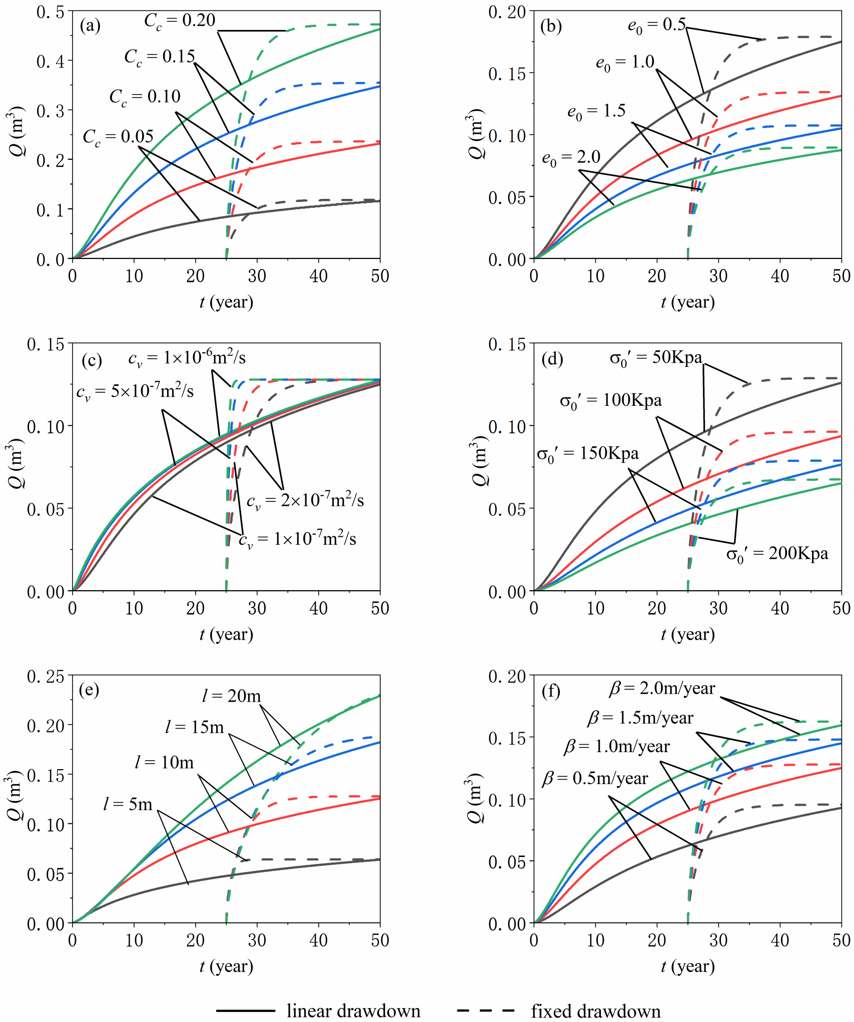

(a)
C_c = 0.20
C_c = 0.15
C_c = 0.10
C_c = 0.05
(b)
e_0 = 0.5
e_0 = 1.0
e_0 = 1.5
e_0 = 2.0
(c)
$c_v = 1\times10^{-6}$m^2/s
$c_v = 5\times10^{-7}$m^2/s
$c_v = 2\times10^{-7}$m^2/s
$c_v = 1\times10^{-7}$m^2/s
(d)
σ_0' = 50Kpa
σ_0' = 100Kpa
σ_0' = 150Kpa
σ_0' = 200Kpa
(e)
l = 20m
l = 15m
l = 10m
l = 5m
(f)
β = 2.0m/year
β = 1.5m/year
β = 1.0m/year
β = 0.5m/year
Q (m^3)
t (year)
linear drawdown
fixed drawdown

Figure 8.

N
1000 km
China
Shanghai
N
Extensometer Group
Jiangsu Province
Chongming Island
Yangtze River
Jiangsu Province
Baoshan District
Jiading District
East China sea
4
Pudong New District
Qingpu District
Urban District
Nanhui District
Songjiang District
Minghang District
Jinshan District
Zhejiang Province
0m 10 20km

Figure 9.

Depth interval (m)	Cross section	Soil types	Unit Weight (kN/m^3)	Void Ratio	Coefficient of Compression(MPa^{-1})	Hydraulic Conductivity(10^{-9}m/s)	Hydrogeological Stratigrapy
0~7		Sand layer one	17.5~19.2	0.83~1.23	0.29~0.65	21500	UA
7~24		Soft clay layer one and two	16.4~19.3	0.70~1.44	0.40~1.50	2.0	Aquitard 1
24~30		Hard clay layer two	20.2	0.66~0.70	0.21~0.35	1.34	Aquitard 1
30~48		Sand layer two	19.1~20.1	0.63~0.81	0.12~0.32	35000	CA1
48~88		Soft clay layer three	18.2~19.3	0.78~1.08	0.34~0.62	2.99	Aquitard 2
88~153		Sand layer three	19.1~21.2	0.43~0.82	0.26~0.45	41000	CA2
153~173		Hard clay layer three	19.7~20.5	0.66~0.86	0.07~0.25	0.13	Aquitard 3
174~239		Sand layer four	18.7~19.3	0.85~0.87	0.25~0.63	18100	CA3
239~333		Hard clay layer four	19.3~20.3	0.59~0.68	0.06~0.41	0.38	Aquitard 4

Figure 10.

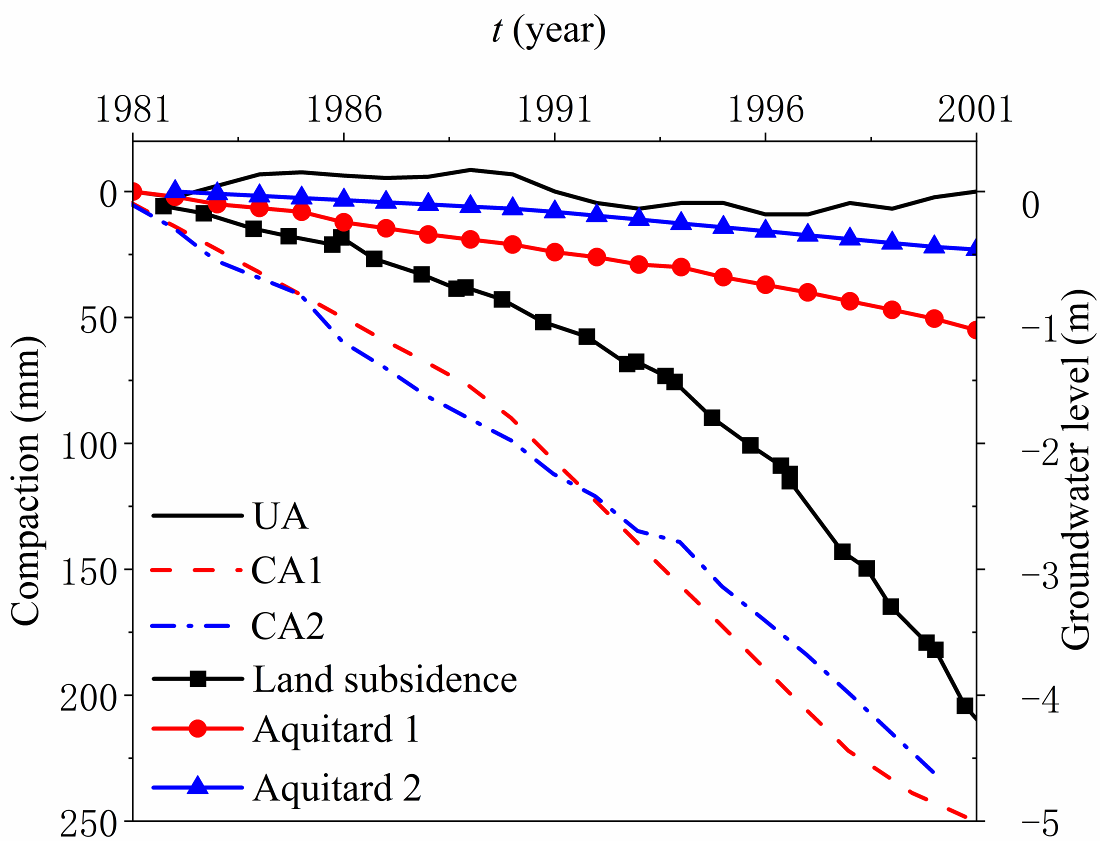

t (year)
1981
1986
1991
1996
2001
Compaction (mm)
0
50
100
150
200
250
Groundwater level (m)
0
−1
−2
−3
−4
−5
UA
CA1
CA2
Land subsidence
Aquitard 1
Aquitard 2

Figure 11.

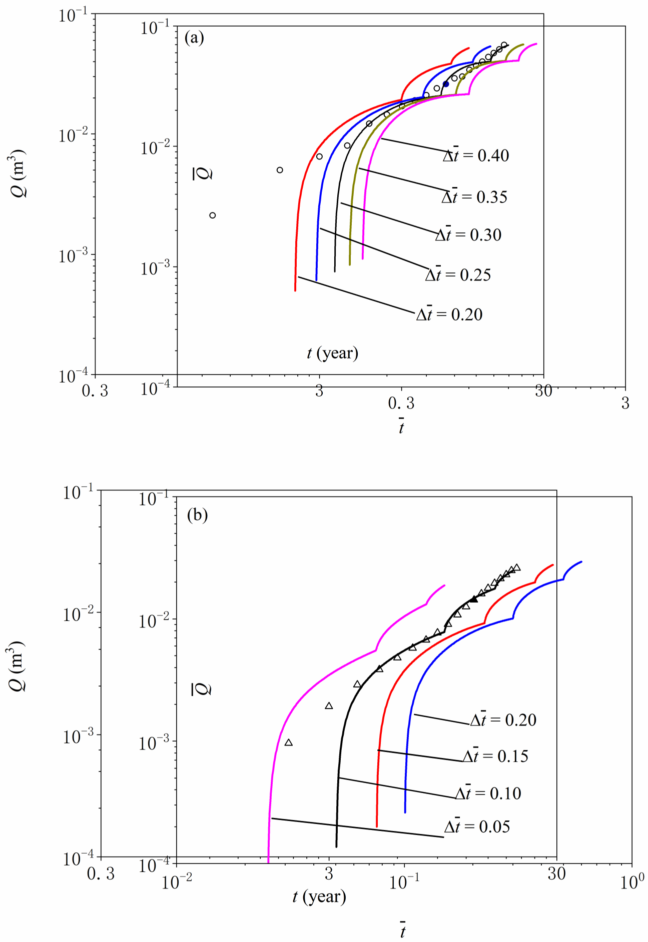

(a)
$\Delta\bar{t}$ = 0.40
$\Delta\bar{t}$ = 0.35
$\Delta\bar{t}$ = 0.30
$\Delta\bar{t}$ = 0.25
$\Delta\bar{t}$ = 0.20
Q (m^3)
$\bar{Q}$
t (year)
$\bar{t}$
(b)
$\Delta\bar{t}$ = 0.20
$\Delta\bar{t}$ = 0.15
$\Delta\bar{t}$ = 0.10
$\Delta\bar{t}$ = 0.05
Q (m^3)
$\bar{Q}$
t (year)
$\bar{t}$

Figure 12.

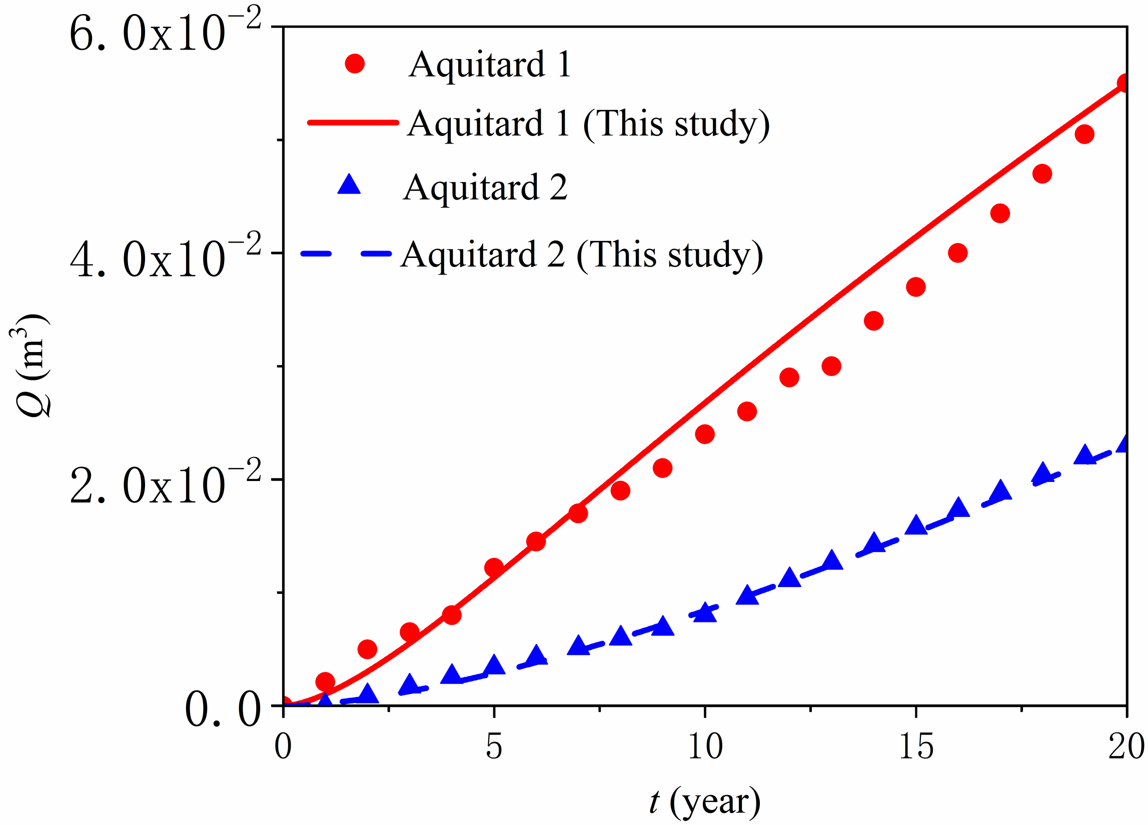

Aquitard 1
Aquitard 1 (This study)
Aquitard 2
Aquitard 2 (This study)
6.0x10^-2
4.0x10^-2
2.0x10^-2
0.0
Q (m^3)
0
5
10
15
20
t (year)

Figure 13.

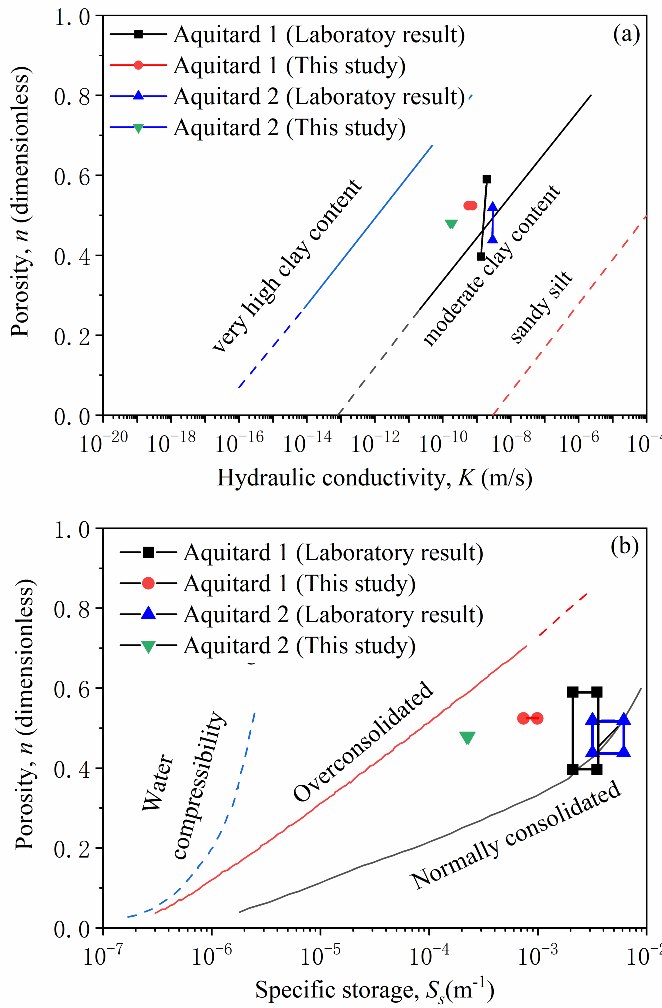
(a)
Aquitard 1 (Laboratoy result)
Aquitard 1 (This study)
Aquitard 2 (Laboratoy result)
Aquitard 2 (This study)
very high clay content
moderate clay content
sandy silt
Porosity, n (dimensionless)
Hydraulic conductivity, K (m/s)
(b)
Aquitard 1 (Laboratory result)
Aquitard 1 (This study)
Aquitard 2 (Laboratory result)
Aquitard 2 (This study)
Water compressibility
Overconsolidated
Normally consolidated
Porosity, n (dimensionless)
Specific storage, Ss(m-1)